

2XMMi J225036.9+573154 – a new eclipsing AM Her binary discovered using XMM-Newton

Gavin Ramsay¹, Simon Rosen², Pasi Hakala³, Thomas Barclay^{1,4}

¹*Armagh Observatory, College Hill, Armagh, BT61 9DG*

²*Department of Physics and Astronomy, University of Leicester, University Road, Leicester LE1 7RH*

³*Tuorla Observatory, University of Turku, Väisäläntie 20, FIN-21500 Piikkiö, Finland*

⁴*Mullard Space Science Laboratory, University College London, Holmbury St. Mary, Dorking, Surrey, RH5 6NT*

19 November 2018

ABSTRACT

We report the discovery of an eclipsing polar, 2XMMi J225036.9+573154, using *XMM-Newton*. It was discovered by searching the light curves in the 2XMMi catalogue for objects showing X-ray variability. Its X-ray light curve shows a total eclipse of the white dwarf by the secondary star every 174 mins. An extended pre-eclipse absorption dip is observed in soft X-rays at $\phi=0.8$ – 0.9 , with evidence for a further dip in the soft X-ray light curve at $\phi \sim 0.4$. Further, X-rays are seen from all orbital phases (apart from the eclipse) which makes it unusual amongst eclipsing polars. We have identified the optical counterpart, which is faint ($r=21$), and shows a deep eclipse (>3.5 mag in white light). Its X-ray spectrum does not show a distinct soft X-ray component which is seen in many, but not all, polars. Its optical spectrum shows H α in emission for a fraction of the orbital period.

Key words: Stars: binary - close; novae - cataclysmic variables; individual: - 2XMMi J225036.9+573154; X-rays: binaries

1 INTRODUCTION

Cataclysmic Variables are accreting binary systems in which a white dwarf accretes material from a late type main sequence star through Roche lobe overflow. If the white dwarf has a significant magnetic field then the formation of an accretion disk can be disrupted or prevented. For white dwarfs with field strengths greater than ~ 10 MG, the accretion stream gets channelled onto the magnetic poles where X-rays are emitted from the post-shock region. The magnetic field also forces the spin period of the white dwarf to synchronise with the binary orbital period. These accreting binaries are called AM Her binaries or polars, since their optical emission is strongly polarised.

The study of polars was transformed with the launch of the X-ray satellite *ROSAT* in 1990. Prior to this, around 17 systems were known. *ROSAT* led directly to the discovery of around 30 new systems (eg Beuermann & Burwitz 1995). It was expected that *XMM-Newton*, launched in 1999, would lead to the discovery of many more such systems. Surprisingly, comparatively few have so far been discovered.

The 2XMM catalogue (Watson et al 2009) gives a description of serendipitous X-ray sources discovered using the EPIC wide-field instruments on board *XMM-Newton*. This was followed by the release of the 2XMMi incremental catalogue which has 17 percent more discrete sources than the

2XMM catalogue. Moreover, each source is accompanied by source specific light curve and spectral products. In this paper we report the discovery of an eclipsing polar, 2XMMi J225036.9+573154, which was found as a result of searching the 2XMMi catalogue for sources which showed variability in their X-ray light curve.

2 XMM-Newton OBSERVATIONS

2.1 The 2XMMi catalogue

The 2XMMi catalogue has associated spectra and light curves that are automatically extracted by the *XMM-Newton* Science Survey Centre pipeline processing software (Watson et al 2001) for sources with more than 500 counts in the EPIC detectors. An assessment of variability in the individual light curves is made by determining χ^2_ν of the data about the mean, and then computing the consequent probability of the constant (null) hypothesis. Those light curves for which this probability is $< 10^{-5}$ are deemed variable. Sources which were possibly compromised by further data quality issues were removed. An initial search of the catalogue found around 400 sources which passed these criteria. The light curves of these sources were visually inspected for periodic behaviour. One source, 2XMMi J225036.9+573154

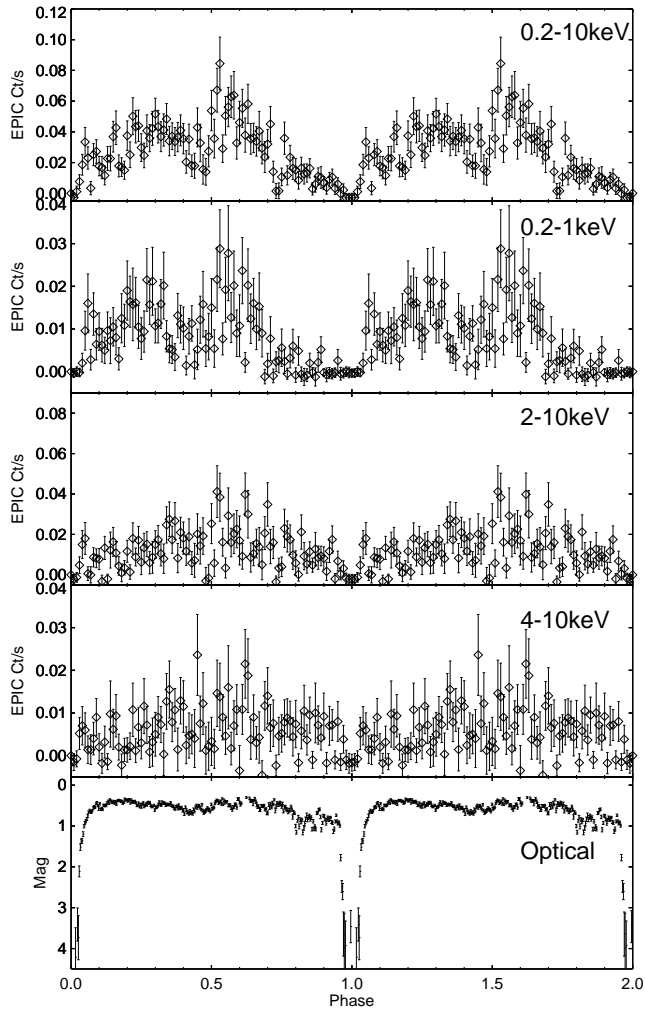


Figure 1. The light curves of XMM J2250+5731 folded on a period of 174.2 mins and $T_0=2454124.245888$ (TT). From the top we show the combined EPIC pn plus EPIC MOS light curve in the 0.2–10keV energy band; the 0.2–1.0keV energy band; the 2–10keV energy band; the 4–10keV energy band (binned into 100 bins) and in the lower panel the white light data obtained using the NOT (the data have been folded but not binned).

(hereafter XMM J2250+5731), was found which showed a characteristic repeating shape on a period of ~ 174 min (Figure 1).

2.2 Pointed observations

XMM J2250+5731 was found in the field of G107.5-1.5 which was observed on 23rd Jan 2007. The EPIC detectors were each configured in full window mode and used the medium filter. The field was observed for a total of 32.9 ksec in the EPIC pn detector and 34.5 ksec in both EPIC MOS detectors. The source was just outside the field of view of the Optical Monitor. Since the source was towards the edge of the EPIC detectors, and there was a nearby ($28''$) X-ray source, XMM J225037.9+573127, which appears to be an active late-type star, we extracted the data from the *XMM-Newton* archive and re-extracted the X-ray light curves and spectra of XMM J2250+5731.

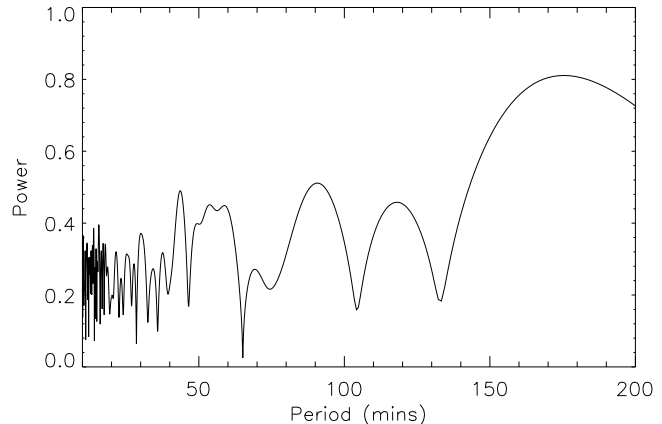


Figure 2. The power spectrum of the combined EPIC (pn plus MOS) 0.2–10keV light curve.

The data were processed using *XMM-Newton* SAS v8.0.1 (released Oct 2008). Only X-ray events which were graded as `PATTERN=0-4` and `FLAG=0` were used. Events were extracted from a circular aperture with $10''$ radius centred on the source, with background events being extracted from source free areas on the same chip as the source. The background data were scaled to give the same area as the source extraction area and subtracted from the source area. (We estimate that the nearby source XMM J225037.9+573127 contributes around 1.5 percent of the flux below 2keV, and a negligible amount at energies above 4keV). To ensure that the spectra were correctly flux calibrated we produced detector spectral response files and ancillary files using the SAS tasks `rmfgen` and `arfgen` respectively.

3 THE X-RAY LIGHT CURVES

We extracted light curves of XMM J2250+5731 in the 0.2–10keV, 0.2–1.0keV, 2–10keV and 4–10keV energy bands from the EPIC pn, EPIC MOS1 and EPIC MOS2 detectors using the method described above. We then obtained a combined light curve for each energy band by adding the separate light curves. Each light curve shows a distinctive sharp drop in intensity every 174 min. This is due to the secondary star eclipsing the accretion region(s) on the white dwarf and represents the binary orbital period. The observation covers 3 eclipses.

We used the standard Lomb-Scargle power spectrum analysis to search for periods in the data (Figure 2). The error on the period was then determined using a bootstrap approach incorporating the generation of synthetic light curves. We find that the period is 0.1210 ± 0.0018 days ($=174.2 \pm 2.6$ mins). We folded the light curve in each of the 4 energy bands on this period and show these light curves in Figure 1.

We have phased the data so that the eclipse, which is total in each energy band, defines $\phi=0.0$. XMM J2250+5731 is relatively faint in X-rays, reaching a peak of ~ 0.08 ct/s in the combined EPIC 0.2–10keV light curve, although this count rate has not been corrected for the source being far off-axis.

Prior to the eclipse, there is a marked decrease in soft

X-ray photons over the phase range $\phi \sim 0.7$ –1.0, compared to those at higher energies. This phenomenon has been seen in other polars (eg Watson et al 1989) and occurs when the accretion stream obscures our view of the hot accretion region located in the upper hemisphere on the white dwarf. Compared to V2301 Oph (for instance, Ramsay & Cropper 2007), the ‘pre-eclipse’ dip seen in XMM J2250+5731 is more extended suggesting that material gets lifted out of the orbital plane over a wider range in azimuth.

At softer energies ($<1\text{keV}$) there is also a dip in the light curve centered at $\phi \sim 0.4$ and with a duration of ~ 0.1 – 0.2 cycles. At higher energies, there is no obvious broad dip at these orbital phases although there are a couple of bins between $\phi=0.4$ – 0.5 which are consistent with zero counts. However, since other bins with negligible flux are also seen at different phases this may just be due to low counting statistics. This dip could either be due to a second dip caused by an accretion stream or it could be due to the rotation of the accretion regions rotating into and out of view as the white dwarf rotates. We will discuss this further in §7.

4 X-RAY SPECTRAL FITS

We extracted spectra from each EPIC detector in the manner described in §2. Initially we extracted spectra using all the available data. However, since the light curves (cf Figure 1) imply the presence of a pre-eclipse dip, we then extracted spectra from the phase interval which was not strongly affected by absorption, ie $\phi \sim 0.05$ – 0.7 . We also exclude the phase interval $\phi=0.38$ – 0.5 which could also be affected by absorption (§3).

In polars, X-rays are generated in a post-shock region at some height above the photosphere of the white dwarf. Since the X-ray spectrum of XMM J2250+5731 has a relatively low signal to noise compared to many polars previously studied using *XMM-Newton* (eg Ramsay & Cropper 2004), we used a simple single temperature thermal bremsstrahlung emission model rather than a more complex (and more physical) stratified cooling flow model (eg Cropper et al 1998, 1999).

We used the *XSPEC* package (Arnaud 1996) to fit the X-ray spectra. We fitted all three EPIC spectra simultaneously and tied the spectral parameters apart from the normalisation parameters. We used the *tbabs* absorption model (the Tübingen–Boulder absorption ISM model, Wilms, Allen & McCray 2000), a single temperature thermal bremsstrahlung component with temperature fixed at $kT = 20\text{keV}$. We added a Gaussian component to account for any emission between 6.4–6.8keV. The spectra along with the best fit ($\chi^2_{\nu}=1.12$) are shown in Figure 3. We show the spectral parameters, the observed and unabsorbed bolometric fluxes in Table 1. Due to the low signal to noise of the spectra, the equivalent width of the Fe $K\alpha$ emission line features was poorly constrained.

In many polars, a strong soft X-ray component ($kT_{bb} \sim 40\text{eV}$) is seen in their X-ray spectra (eg Ramsay et al 1994, Beuermann & Burwitz 1995). This is due to the hard X-rays irradiating the photosphere of the white dwarf which are then re-emitted as soft X-rays. The standard accretion model predicts that $L_{\text{soft}}/L_{\text{hard}} \sim 0.5$, where L_{soft} and L_{hard} are the luminosities of the soft and hard X-ray

N_H	$3.4^{+2.2}_{-1.8} \times 10^{20} \text{ cm}^{-2}$
Flux ^o EPIC pn	$3.5^{+0.3}_{-0.4} \times 10^{-13} \text{ erg s}^{-1} \text{ cm}^{-2}$
Flux ^o EPIC mos1	$2.8^{+0.4}_{-0.4} \times 10^{-13} \text{ erg s}^{-1} \text{ cm}^{-2}$
Flux ^o EPIC mos2	$2.1^{+0.4}_{-0.3} \times 10^{-13} \text{ erg s}^{-1} \text{ cm}^{-2}$
Flux ^u EPIC pn	$8.1^{+0.9}_{-1.0} \times 10^{-13} \text{ erg s}^{-1} \text{ cm}^{-2}$
Flux ^u EPIC mos1	$6.4^{+1.0}_{-0.9} \times 10^{-13} \text{ erg s}^{-1} \text{ cm}^{-2}$
Flux ^u EPIC mos2	$4.8^{+0.9}_{-0.8} \times 10^{-13} \text{ erg s}^{-1} \text{ cm}^{-2}$
χ^2_{ν}	1.12 (34 dof)

Table 1. The spectral fit to the EPIC pn, MOS1 and MOS2 spectra extracted from $\phi=0.05$ – 0.7 . Flux^o refers to the observed flux measured over the 0.2–10keV energy band and Flux^u refers to the unabsorbed bolometric flux.

components respectively (Lamb & Masters 1979, King & Lasota 1979). Although the energy balance in polars was a source of great debate for many years, Ramsay & Cropper (2004) showed that the majority of polars in a high accretion state have X-ray spectra which are in good agreement with the standard model.

To see if such a soft X-ray component could be ‘hidden’ by the moderate level of absorption (cf Table 1) we added a blackbody with a range of different temperatures. We fixed its normalisation so that the implied ratio, $L_{\text{soft}}/L_{\text{hard}} \sim 0.5$. Since the soft X-rays are optically thick, and hence the intrinsic soft X-ray luminosity is viewing angle dependant, we assumed a viewing angle of 45° for argument. If we just consider the X-ray data, we find a blackbody with temperature less than $kT \lesssim 20\text{eV}$ can easily be hidden.

We were fortunate in being able to obtain a short observation of the field of XMM J2250+5731 using *Swift* on the 3rd and 4th Dec 2008. Observations using the UV Optical Telescope (Roming et al 2005) were made using the UVW2 filter (peak effective wavelength 2120Å). XMM J2250+5731 was not detected, and we estimated a 3σ upper limit of $\sim 2.4 \times 10^{-17} \text{ erg s}^{-1} \text{ cm}^{-2} \text{ Å}^{-1}$. If we assume a blackbody of different temperatures and with a normalisation such that $L_{\text{soft}}/L_{\text{hard}} \sim 0.5$, we find that a blackbody of $kT \sim 5$ – 20eV can be present and not detected in the near UV or soft X-ray energy ranges. (Although a handful of X-ray events were detected near the source position of XMM J2250+5731, they were too low to derive any meaningful information).

The unabsorbed bolometric flux implies an X-ray luminosity of $\sim 8 \times 10^{29} d_{100}^2 \text{ erg/s}$, where d_{100}^2 is the distance in units of 100 pc. Ramsay & Cropper (2004) found that the mean bolometric luminosity in their sample of polars observed in a high state using *XMM-Newton* was $\sim 2 \times 10^{32} \text{ erg/s}$. In the next section we find that XMM J2250+5731 shows a range in optical brightness over the longer term and therefore a range of accretion states (a general characteristic of polars). Assuming that XMM J2250+5731 was observed in a high accretion state at the epoch of the *XMM-Newton* observations we find that in order that XMM J2250+5731 has an X-ray luminosity consistent with other polars in a high state it must lie at a distance of ~ 1.5 – 2.0 kpc. With Galactic co-ordinates of $l = 107.2^\circ$ and $b = -1.6^\circ$, this places XMM J2250+5731 close to the Perseus spiral arm (Xu et al 2005).

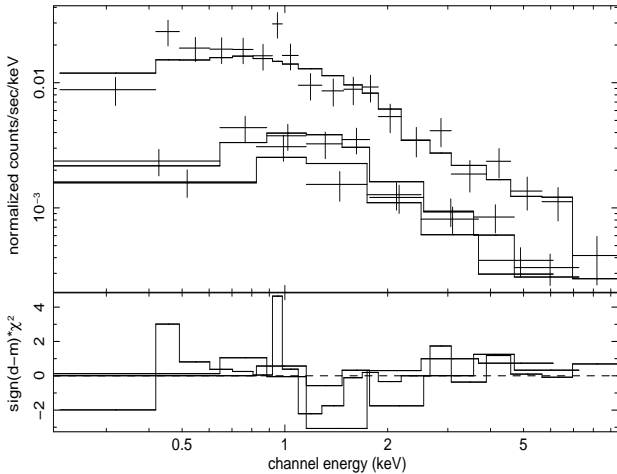


Figure 3. Upper Panel: The EPIC spectra extracted from the bright phase interval along with the best fits (the upper most spectrum is that derived from the EPIC pn, while the lower ones are derived from the EPIC MOS 1 and 2 detectors). Lower Panel: the residuals to the best fit are shown in units of χ^2 .

5 OPTICAL PHOTOMETRY

To locate the optical counterpart of XMM J2250+5731 we obtained optical photometry using ALFOSC on the Nordic Optical Telescope (NOT) located on La Palma during 28th Sept 2008. Each exposure was in ‘white light’ and 15 sec in length, with another 5 sec of readout time, resulting in 2.9 h of data in total. Each source in the field (Figure 4) was searched for variability. One source showed a clear eclipse lasting for ~ 12 mins and a depth $\gtrsim 3.5$ mag (Figure 1). This is the optical counterpart to XMM J2250+5731 and its co-ordinates are $\alpha_{2000} = 22^h 50^m 36.97^s$, $\delta_{2000} = +57^\circ 31' 54.2''$ (which is within $0.8''$ of the X-ray position).

We searched the IPHAS catalogue (Drew et al 2005) which surveyed the northern galactic plane in $r, i, H\alpha$ filters to determine if the optical counterpart of XMM J2250+5731 was detected in this survey. We find that IPHAS gives $r = 20.32 \pm 0.05$, $i = 20.1 \pm 0.2$, $H\alpha = 19.69 \pm 0.09$ for XMM J2250+5731. All sources within a $30''$ radius of the X-ray position were extracted. XMM J2250+5731 is at the extreme blue end in the $(r - i)$ distribution and consistent with the location of the CVs found in IPHAS data in the $(r - i)$, $(r - H\alpha)$ colour-colour plane (cf fig1 of Corradi et al 2008).

We also obtained U, g, R images of XMM J2250+5731 using the Wide Field Camera on the Isaac Newton Telescope on 6th Nov 2008: Figure 4 shows the g band image of the immediate field. Using standard star observations taken immediately before these observations we find that $U = 21.75 \pm 0.11$, $g = 21.16 \pm 0.05$ and $r = 21.53 \pm 0.05$. Compared to other stars in the field, it is clearly blue and appears to be more than 1 mag fainter than found at the epoch of the IPHAS pointings. This is not unexpected since polars are known to show different accretion states.

6 OPTICAL SPECTROSCOPY

We obtained spectra of XMM J2250+5731 using the 4.2m William Herschel Telescope and the Intermediate dispersion Spectrograph and Imaging System (ISIS) on La Palma on

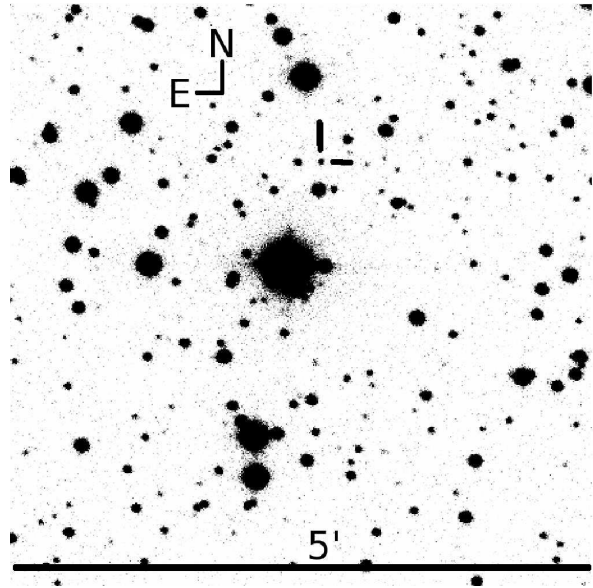


Figure 4. The finding chart of XMM J2250+5731 extracted from a g band image taken with the INT WFC on 6th Nov 2008.

6th Oct 2008. We used the R300B and R158R gratings giving a spectral resolution of $\sim 2.5\text{\AA}$ and $\sim 5\text{\AA}$ respectively. The seeing was $\sim 0.8''$ and the slit was set to match the seeing. We took 16 spectra in both the red and blue arms.

With an out of eclipse brightness of $r \sim 21$, each individual spectrum was of low signal to noise. Moreover, in the blue arm, there was electronic noise in the images, the pattern of which varied from image to image. This coupled with the low signal to noise of the spectra prevented us from extracting any useful information from the blue arm. In the red arm, we were able to extract a spectrum from each image. For 9 sequential spectra we were able to detect $H\alpha$ in emission. We show the mean of these spectra in Figure 5. For the remaining 7 spectra for which we did not detect $H\alpha$ in emission we attribute this to the fact that the observations occurred during the phase interval of the pre-eclipse absorption dip or that the accretion stream was presenting a small surface area at those phase intervals. (Given the error on the orbital period, §3, the phasing of the WHT spectra using the NOT photometric observations as a marker of the phasing is uncertain by approximately one orbital cycle).

7 DISCUSSION

7.1 The X-ray light curve

In polars, it is thought that the magnetic axis of the white dwarf is tilted towards the secondary star, but shifted a few 10 's of degrees ahead in azimuth (as the binary rotates) of the line of center joining the two stars (eg Cropper 1988). It is therefore the accretion region in the upper hemisphere which is obscured by the accretion flow during the pre-eclipse absorption dip.

Eclipsing polars have long been the target of dedicated X-ray observations. Many of these polars show a distinct bright and faint phase as the accretion region rotates into

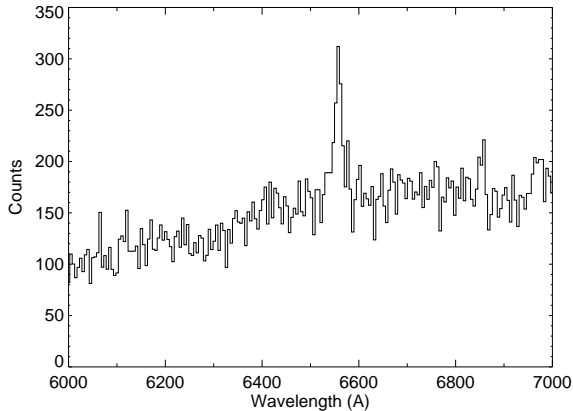


Figure 5. In 9 out of our 16 spectra taken of XMM J2250+5731 using the WHT and ISIS in Oct 2008, we detected the H α emission line. This figure shows the mean of these 9 spectra. ISIS and the WHT on 6th Oct 2008. The flux scale is arbitrary.

view and out of view and many show a characteristic pre-eclipse absorption dip. In these systems there is no evidence for a second accretion pole. One of the few eclipsing polars to show emission throughout the binary phase is V2301 Oph (Ramsay & Cropper 2007). We find that in the case of XMM J2250+5731, X-ray emission is also seen throughout the orbital phase. We attempted to invert the X-ray light curves and map the X-ray regions on the white dwarf using an approach similar to that of Cropper & Horne (1994). However, because of the relatively low signal to noise of the data we could not identify a unique solution.

In §3 we noted the presence of a broad dip in soft X-rays at $\phi \sim 0.4$ which could be attributed to either an accretion stream (since there is no similar feature at higher energies) or the rotation of the accretion region(s) as they come into and out of view. In the former case, the dip could be due to a second accretion stream obscuring our line of sight to the accretion region located in the lower hemisphere of the white dwarf. To our knowledge this would make XMM J2250+5731 unique amongst polars in showing two absorption dips. In the latter case, the change in the soft X-ray light curve could be due to either the rotation of two accretion regions, located in opposite hemispheres, or the rotation of one relatively large polar region. (Our inversion maps showed that both scenarios could re-produce the soft X-ray light curves). The fact that soft X-rays emitted at the base of the accretion region are optically thick and hence viewing angle dependant could account for the change in the soft X-ray flux. In contrast, the harder X-rays are optically thin and therefore not viewing angle dependant.

Optical polarimetry data would be able to confirm the presence of two accretion poles. However, since XMM J2250+5731 is rather faint, this may prove challenging.

7.2 The energy balance

Ramsay & Cropper (2004) presented the results of a snapshot survey of polars observed in a high accretion state using *XMM-Newton*. They found that 7 out of 21 systems did not show a distinct soft X-ray component. Vogel et al (2008) also report that 2XMMp J131223.4+173659,

which was discovered serendipitously using *XMM-Newton*, does not show a soft X-ray component. We have searched the literature for further observations of polars observed using *XMM-Newton* in a high state: we find an additional 6 polars. (We are aware of a number of observations of polars in the high state which have been carried out but have not as of yet been published). V1309 Ori (Schwarz et al 2005), V1432 Aql (Rana et al 2005) and SDSS J075240.45+362823.2 (Homer et al 2005) all show distinct soft X-ray components while SDSS J072910.68+365838.3 and SDSS J170053.30+400357.6 (Homer et al 2005) do not. In the case of SDSS J015543.4+002807.2 (Schmidt et al 2005) the existence of a soft component is not required at a high significance and hence we define it as not having a soft X-ray component. We therefore find that 10 out of 27 systems observed in a high state do not show a distinct soft X-ray component.

Ramsay & Cropper (2007) suggested that if the temperature of the re-processed X-rays was low enough, it would not be observable using the *XMM-Newton* X-ray detectors. This view is also supported by the analysis carried out by Vogel et al (2008) on observations of 2XMMp J131223.4+173659. The reason for this could be that the accretion flow covers a larger fraction of the photosphere of the white dwarf or that the mass accretion rate is lower than in systems which showed a soft component (since $kT_{bb} \propto (\dot{M}/f)^{1/4}$, where \dot{M} is the mass accretion rate and f is the fractional area over which accretion is occurring).

There is no obvious reason as to why some polars would have accretion occurring over a larger area than others: they share no common characteristics such as magnetic field strength or orbital period. Indeed, as noted by Ramsay & Cropper (2004) two systems (BY Cam and RX J2115–58) have one pole which shows a soft component and one pole which does not. Further, three systems which have at least one pole which does not show a soft component are asynchronous systems. However, V1432 Aql which does show a soft component is also an asynchronous polar.

8 CONCLUSIONS

We have serendipitously discovered a faint polar, XMM J2250+5731, with an orbital period of 2.9 h, in the 2XMMi catalogue. We have identified the optical counterpart as a $r \sim 21$ object and it shows a deep eclipse in the optical and X-ray bands lasting ~ 12 mins. At soft X-ray energies there is a distinctive drop in counts starting ~ 0.3 cycles before the eclipse. This is due to the accretion stream obscuring the accretion region in the upper hemisphere of the white dwarf. A second dip is seen in soft X-rays at $\phi \sim 0.4$ which could either be due to obscuration of the accretion region by a second stream or due to the rotation of the accretion region(s) rotating into and out of view. Amongst eclipsing polars, XMM J2250+5731 is unusual in that X-ray emission is visible over the whole of the binary orbital phase, apart from the eclipse.

We have analysed the X-ray spectrum of XMM J2250+5731 and find no evidence for a distinct soft X-ray component. Of the 27 polars which have been observed using *XMM-Newton* and found to be in a high accretion state, 10 show no distinct soft X-ray component. This is a surpris-

ingly high fraction. This together with the result that only a small fraction of polars show a soft X-ray excess (Ramsay & Cropper 2004), changes our whole perception of polars being strong soft X-ray sources. Further, it suggests that polars with strong soft X-ray components were preferentially discovered using *EXOSAT*.

9 ACKNOWLEDGEMENTS

Based on observations obtained with *XMM-Newton*, an ESA science mission with instruments and contributions directly funded by ESA Member States and NASA. We thank Gillian James for providing an initial reduction of the *XMM-Newton* data and Diana Hannikainen and Hanna Tokola for assisting with the NOT observations. Observations were made using the William Herschel Telescope, the Isaac Newton Telescope and the Nordic Optical Telescope on La Palma. We gratefully acknowledge the support of each of the observatories staff. We also thank Andrew Beardmore and other members of the *Swift* team for scheduling observations of our target. Some of the data presented here have been taken using ALFOSC, which is owned by the Instituto de Astrofísica de Andalucía (IAA) and operated at the Nordic Optical Telescope under agreement between IAA and the NBIFAFG of the Astronomical Observatory of Copenhagen.

REFERENCES

- Arnaud, K. A., 1996, *Astronomical Data Analysis Software and Systems V*, eds Jacoby, G., Barnes, J., p17, ASP Conf Series, 101
- Beuermann, K., Burwitz, V., 1995, In ASP Conf Series, 85, 99
- Corradi, R. L. M., et al, 2008, *A&A*, 480, 409
- Cropper, M., 1988, *MNRAS*, 231, 597
- Cropper, M., Horne, K., 1994, *MNRAS*, 267, 481
- Cropper, M., Ramsay, G., Wu, K., 1998, *MNRAS*, 293, 222
- Cropper, M., Wu, K., Ramsay, G., Kocabiyik, A., 1999, *MNRAS*, 306, 684
- Drew, J., et al, 2005, *MNRAS*, 362, 753
- Homer, L., et al, 2005, *ApJ*, 620, 929
- King A. R., Lasota J. P., 1979, *MNRAS*, 188, 653
- Lamb D. Q., Masters A. R., 1979, *ApJ*, 234, 117
- Ramsay, G., Mason, K. O., Cropper, M., Watson, M. G., Clayton, K. L., 1994, *MNRAS*, 270
- Ramsay, G., Cropper, M., 2004, *MNRAS*, 347, 497
- Ramsay, G., Cropper, M., 2007, *MNRAS*, 379, 1207
- Rana, V. R., Singh, K. P., Barrett, P. E., Buckley, D. A. H., 2005, *ApJ*, 625, 351
- Roming, P. W. A., et al, 2005, *Space Sci Rev*, 120, 95
- Schmidt, G. D., et al, 2005, *ApJ*, 620, 422
- Schwarz, R., Reinsch, K., Beuermann, K., Burwitz, V., 2005, *A&A*, 442, 271
- Vogel, J., Byckling, K., Schwope, A., Osborne, J. P., Schwarz, R., Watson, M. G., 2008, *A&*, 485, 787
- Watson, M. G., King, A. R., Jones, M. H., Motch, C., 1989, *MNRAS*, 237, 299
- Watson, M. G., et al, 2001, *A&A*, 365, L51
- Watson, M. G., et al, 2009, *A&A*, 493, 339
- Wilms, J., Allen, A., McCray, R., 2000, *ApJ*, 542, 914
- Xu, Y., Reid, M. J., Zheng, X. W., Menten, K. M., 2006, 311, 54